

LITHOLOGICAL MAPPING AND LINEAMENT ANALYSIS IN ZARIA AND ITS ENVIRONS USING REMOTE SENSING TECHNIQUE

BY

Ishaku, Y.M. and Abubakar, Y.I.*

Department of Geology, Ahmadu Bello University, Zaria
Corresponding Author's Email: iayusuf@abu.edu.ng

ABSTRACT

The study area is underlain by Precambrian rocks which lie in the mobile zone between the West African and Congo Craton. Detail remote sensing analysis was carried out using landsat ETM⁺ data set and SRTM DEM to map lithological units and understand regional structural pattern of the study area. Lithological and structural map of the area was produced using a false colour composite image from band 7, 4 and 1 in RGB. Three main lithological units were mapped in the area include older granite, biotite gneiss and metasedimentary rocks. Lineament analysis was carried through a semi-automatic process. Result indicates variations in lithological units and revealed a dominant NW-SE trend accompanied by a less dominant N-S and E-W direction. Lineament length ranged from 0.807km to 10.0535km. Areas of high lineament length are observed in the North and Southern part of the study area. The mean lineament length ranges from 0.6-0.9km. Correlation between lineament length and orientation show a close correlation between NW-SE and NE-SW, and NE-SW and E-W lineament specie. From the lineament density map, areas of extremely high lineament density are located in the western part occupying an area extent of 2.90km², very high lineament density occurs in the eastern to northern to southeastern parts and has an area extent of 26.73km², high lineament density occur in the western, south eastern and c north central parts of the study area, occupying an area extent of 150.4 km² and low density has an area extent of 329.2km². Areas of short lineament length cover a total area of 387.3km². Areas of very short lineaments cover a total area of 104km², while extensive lineament length covers a surface area of 217.7km². The present study has shown that ETM⁺ and SRTM DEM are powerful tools in lithological and lineament mapping and can be effectively used in reconnaissance study. There is no standard on selection of the optimum band for manual lineament extraction. Therefore, it is recommended that the geologic, topographic properties and vegetation cover of the selected area should be taken into the consideration.

Key words: ETM⁺, Lineament, Lithological Mapping, Remote Sensing, SRTM DEM, Zaria

INTRODUCTION

In the past years, geological mapping was performed through fieldwork i.e. traversing, but nowadays new techniques which are efficient in terms of time and money have been introduced to work together with traditional geological mapping.

Acquisition of data by remote sensing is among the technological advancement that has been realized, and in geological aspect, the technique is normally used in acquiring Earth's surface geological data, for instance structural features, lithologies, lithological sequences, relative age of rock strata, types of drainage pattern, soil type, vegetation cover etc (Drury, 1993). This technique when used together with field check or ground truthing, makes geological mapping more effective and efficient in all aspects of cost.

The identification of geological and structural features is difficult in remote sensed image because different surface conditions such as vegetation, agricultural activities and weathering crust may act as hindrance to geological and structural signals (Drury, 1993). Thus it is therefore essential to assess the applicability of individual remote sensing techniques as well as other factors to remove errors and noises before any interpretation of remote sensing data. Removal of noise and cloud cover effects can well be performed through special techniques such as filtering found in remote sensing software. For the case of geological analysis band rationing is a prominent method in reducing haze and vegetation cover effects (Carranza, 2002). Near infrared (NIR), mid-infrared (MIR) and shortwave infrared (SWIR) electromagnetic windows in remote sensing are very useful in geological analysis. Example, for the Landsat thematic mapper (TM) data, band-5 and band-7 have been proved to be more successful in discriminating different rock types and effective in identifying zones of hydrothermal alteration (Crosta and Moore, 1989; Drury, 1993; Carranza and Hale, 1999; Ferrier *et al.* 2002; Crosta and Filho, 2003; Moore, Hoffmann and Glenn, 2007).

Some part of the study area has rugged terrain which makes it inaccessible, and hence it becomes necessary to use alternative data such as remote sensing to map such areas. The aim of this study is to utilize remote sensing techniques to map the lithology and lineament of Zaria and its environs in order to assess its usefulness in mapping the lithological unit and analyzing lineament in the study area.

Geology of the Study Area

Nigeria lies west of the West African craton in the region of late Precambrian to early Paleozoic orogenesis (Olusiji, 2013). The Geology of Nigeria is dominated by crystalline and sedimentary rocks both occurring approximately in equal proportions (Woakes *et al* 1987)

The study area falls within the northern sector of the Nigerian basement complex. Details of the geology of the sector are contained in McCurry (1976). The study area lies between Latitudes N11⁰ 00' and N11⁰ 15' and Longitudes E7⁰ 30' and E7⁰ 45' which comprises Zaria and its environs covering an estimated area of about 27,750 km² (Figure 1). It is completely underlain by the basement rocks which form part of the Paleozoic basement complex of Nigeria. The second deformation phase being more intense than the first almost obliterated the former leaving a dominant North-South structural trend. Major transcurrent faulting and the development of a system of joints followed the second deformation phase. The intense regional tectonism that preceded and accompanied the emplacement of Older Granite during the later phases of the second cycle called Pan-African orogeny produced a well-defined and extensive North-South trend in the north central Nigeria, including Zaria area (Ike, 1974). The author also reported the

existence of 159 numerous joints, fractures, and faults within his study area in Zaria Granite batholiths in which a major NE-SW shear-fault complemented by numerous NW-SE shear-faults were emphasized. Further, McCurry (1973) identified the Basement Complex rocks of Nigeria as underlying the geology of sheet 102SW Zaria, where study area lies. Rock types of the northern Nigeria Basement Complex are classified into three (3) namely the migmatite gneiss complex, Younger Metasediment and the Older Granites.

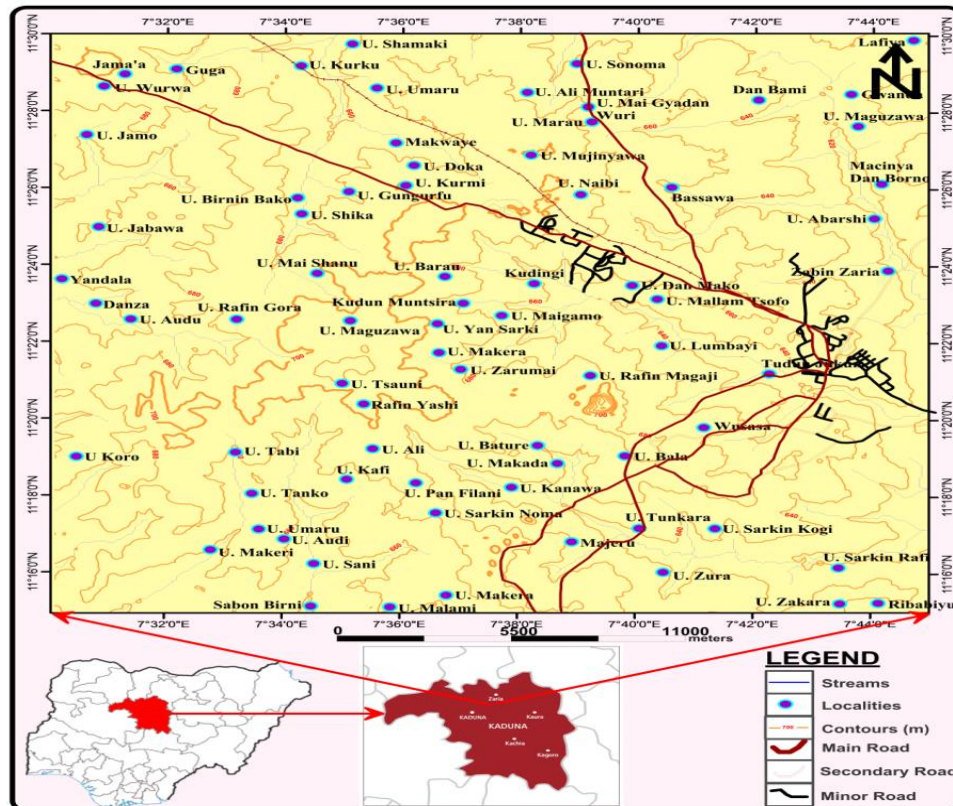


Figure 1: Location Map of the Study Area

MATERIALS AND METHODS

A single scene of Landsat Enhanced Thematic Mapper plus (ETM+) 2005-10-30, path 186/ Row 053 acquired on 30-10-2005 was downloaded from the global land facility cover University of Maryland USA. The data has seven bands sensitive to different wavelength. Six of these bands detect visible (7, 4, 1), near infrared “NIR” (3) and short wave infrared “SWIR” (5), a thermal and panchromatic (single band image generally displayed as shades of gray). Lineament analysis was carried out using SRTM DEM images. The area of study was subset from the single scene and was used in the present study.

One of the characteristic features of the satellite images is a parameter called spatial frequency which is defined as the number of changes in brightness value per unit distance for any particular part of an image. If there are very few changes in brightness value over a given area in an image, this is referred to as a low-frequency area. Conversely, if the brightness values change

dramatically over short distances, this is an area of high frequency detail (Jensen, 1996). Therefore, filtering operations are used to emphasize or deemphasize spatial frequency in the image. This frequency can be attributed to the presence of lineaments in the area. In other words, the filtering operation will sharpen the boundary that exists between adjacent lithological units. Directional filters (edge detection filters) are designed to enhance linear features such as roads, streams, faults, etc. The filters can be designed to enhance features which are oriented in specific directions. Commonly used edge detection filters are Gradient- Sobel, and Gradient-Prewitt.

ENVI 4.5 was used to process landsat images to enhance lithological units. A false colour composite was used to display variations in lithological units. The lithological units were being confirmed by field work. Lineament analysis was carried out using SRTM DEM images due to its high resolution. Eight shaded relief images were produced by changing the azimuth direction. This method has huge advantage because it enables lineaments to be extracted from a multi directional source thus extracting some lineaments which will be hidden when using a unidirectional method.

ERDAS imagine was used to produce shaded relief images. An ambient light setting of 0.20 was used to ensure good contrast. Also a solar elevation of 30° was chosen. Shaded relief images were created by varying the azimuth (sun angle). Eight shaded relief images were created from the following azimuth; 0° , 45° , 90° , 135° , 180° , 225° , 270° and 315° . After generation of shaded relief images, shaded relief images with azimuth 0° , 45° , 90° and 135° were combined to produce a single shaded relief images. Equally, shaded relief images azimuth 180° , 225° , 270° and 315° were combined to produce another shaded relief image.

Generation of shaded relief images was followed by automatic lineament extraction using PCI Geomatica software. Extraction of lineaments was done using parameters. Level of coincidence analysis was performed to in order to understand the similarities existing between lineaments extracted from the two combined shaded relief images.

The buffer analysis is a technique by which a lineament is fracture correlated if fractures in bedrock outcrops have strikes similar to the trend of an individual lineament within a specified “buffer” zone, around each lineament. Those lineaments whose buffers contain at least one steeply dipping fracture (greater than 45°) and have a trend within ± 50 of the strike of the fracture are classified as “fracture correlated”. To perform a level of coincidence analysis buffering of lineaments extracted from both shaded relief images was performed. Buffering of shaded relief images was first done followed by reclassification of buffered images into two classes.

Using raster calculator tool in Arc GIS, the reclassified buffered images were combined to generate a level of coincidence image. Since the reclassified buffered images were binary the level of coincidence for this image has a maximum of eight and a minimum of zero. Level of coincidence of eight indicates areas where lineaments appeared on all eight images. While level of coincidence of zero represents areas with no lineaments. After reclassification, both reclassified images were added to produce a thematic image showing the level of co-incidence (level of acceptance) of both images.

Images were classified into two classes. Classes close to the lineaments were given weight value of one and classes further away from the lineaments were given weight values of zero. The level of coincidence image was then reclassified into a binary image. Observing this image area with

white pixels represents areas with presence of lineaments while an area with dark pixels represents areas with absence of lineaments. In order to enhance this level of acceptance, reclassification of level of coincidence image into two classes was performed. Manual digitization was performed on the coincidence reclassified image to produce a final lineament map of the study area. Production of final lineament map was followed by statistical analysis of lineaments.

Lineaments lengths, density and intersection were determined using statistical analysis. The lineament lengths were plotted in Grapher 4 Excel spread sheet to generate rose diagram. The Rose diagram shows prominent lineaments trends direction. Lineament length shows Positive skewness which is an indication that most lineaments in the study area are not extensive. The lineament density is an indicator for the degree of rock fracturing. High lineament densities are identified as zones of high degree of rock fracturing.

RESULTS AND DISCUSSION

Lineament Analysis

Lineament analysis was carried out using Shuttle topography mission digital elevation model (SRTM DEM). Using Erdas Imagine software, Shaded relief images were generated by varying the solar azimuth through angle 0° , 45° , 90° , 135° , 180° , 225° , 270° and 315° (Figures 2-4). An ambient light setting of 0.2 and a solar elevation of 30° was chosen to ensure good contrast.

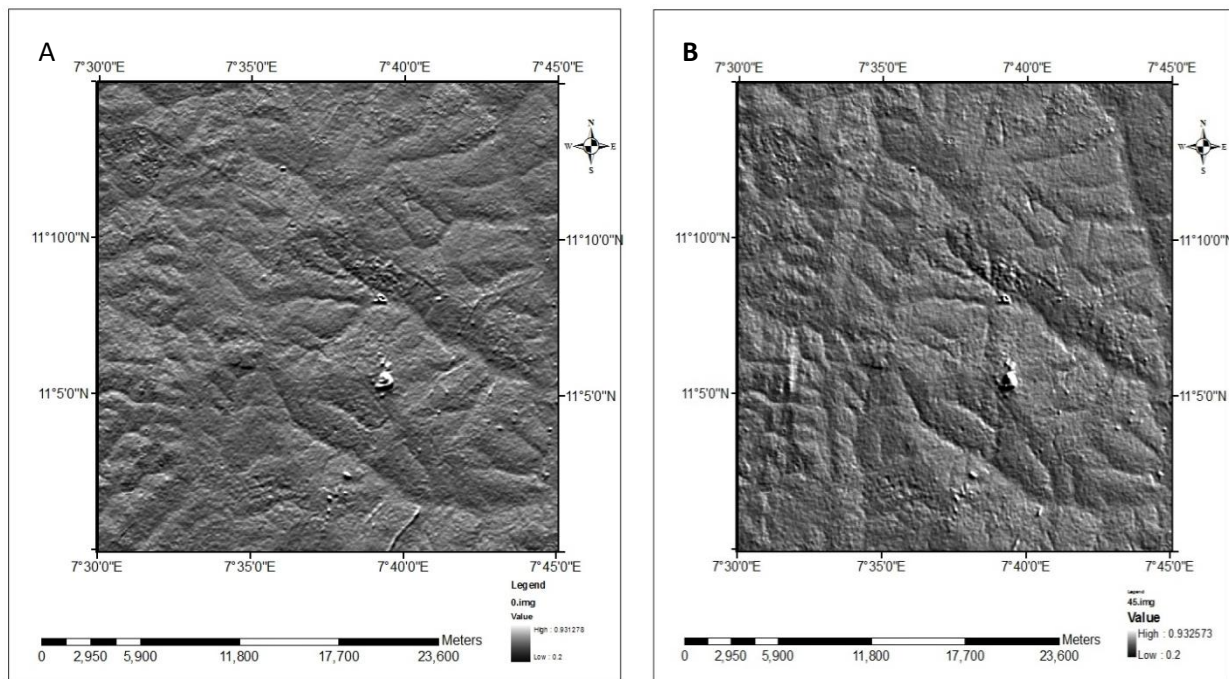


Figure 1: Shaded Relief Images of the Study Area A = 0° , B = 45° (From present work)

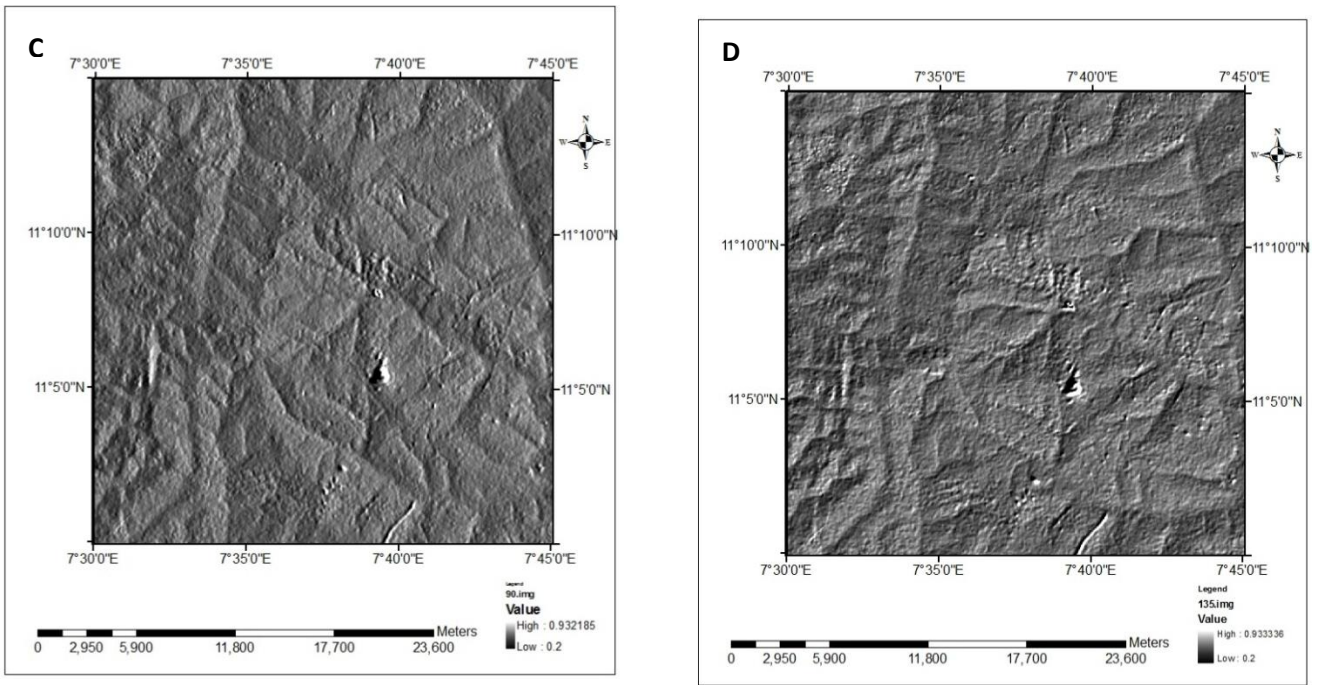


Figure 2: Shaded Relief Images of the Study Area C = 90°, D = 135° (From present work)

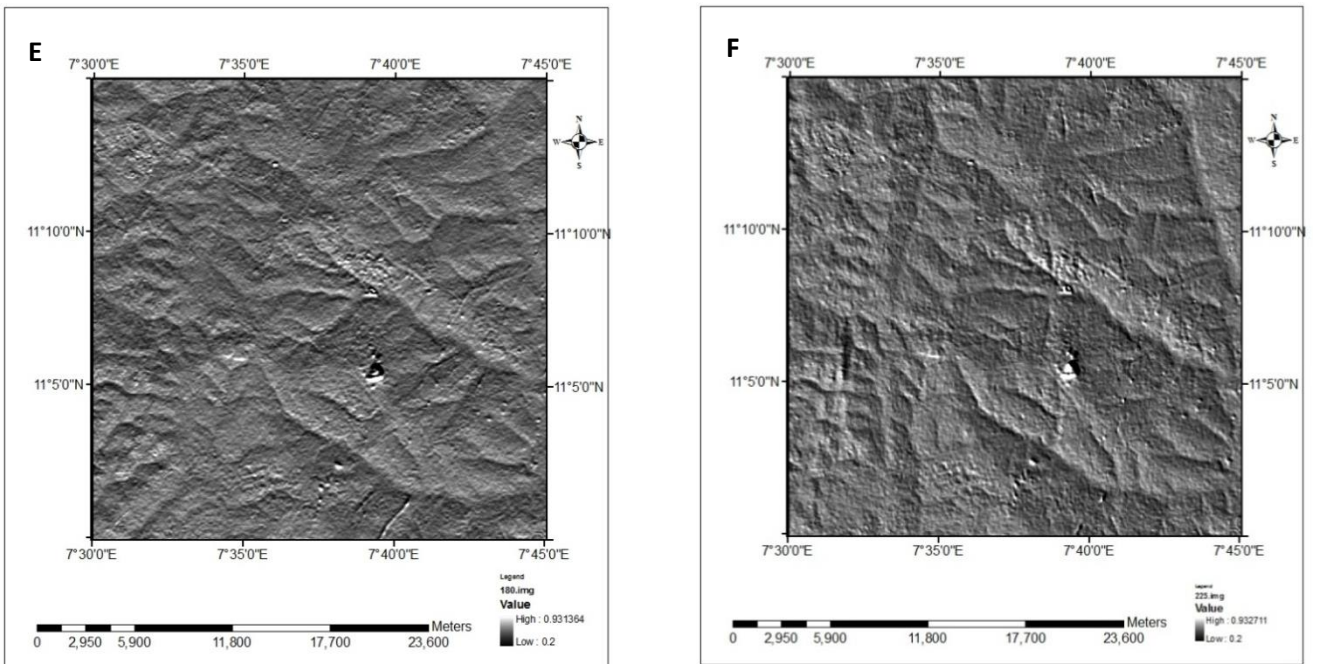


Figure 3: Shaded Relief Images of the Study Area E=180°, F = 225° (from present work)

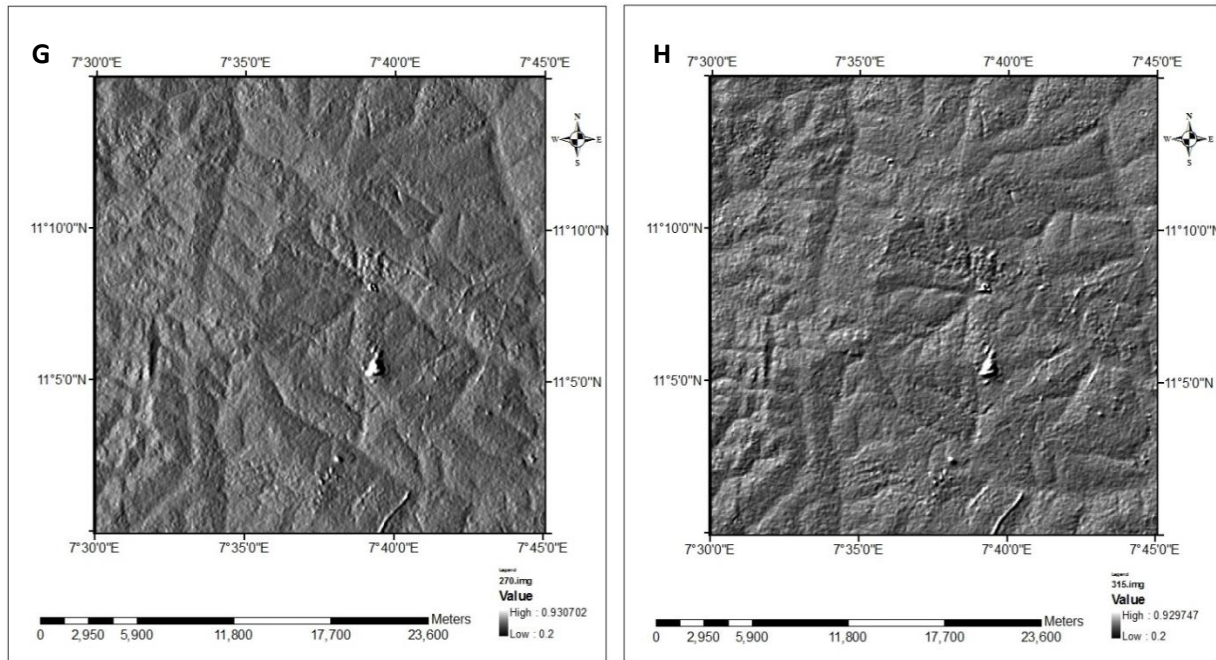


Figure 4: Shaded Relief Images of the Study Area G = 270⁰, H = 315⁰ (From present Work)

Production of shaded relief images was followed by combining shaded relief images with azimuth direction 0, 45, 90, 135 and 180, 225, 270, 315 to produce a combine shaded relief image 1 and 2 (Figure 5).

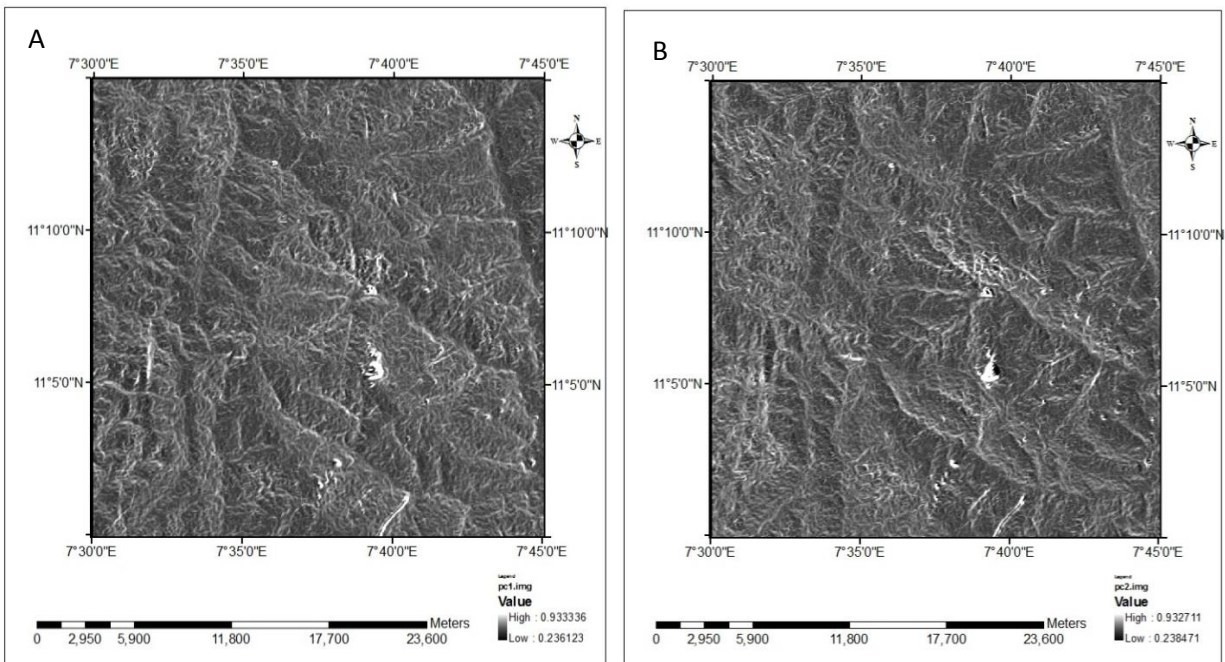


Figure 5: Combined Shaded Relief Images A = (0, 45, 90, 135), B= (180, 225, 270, 315)

PCI Geomatica was used to automatically extract lineaments from the combined shaded relief images (Figure 6).

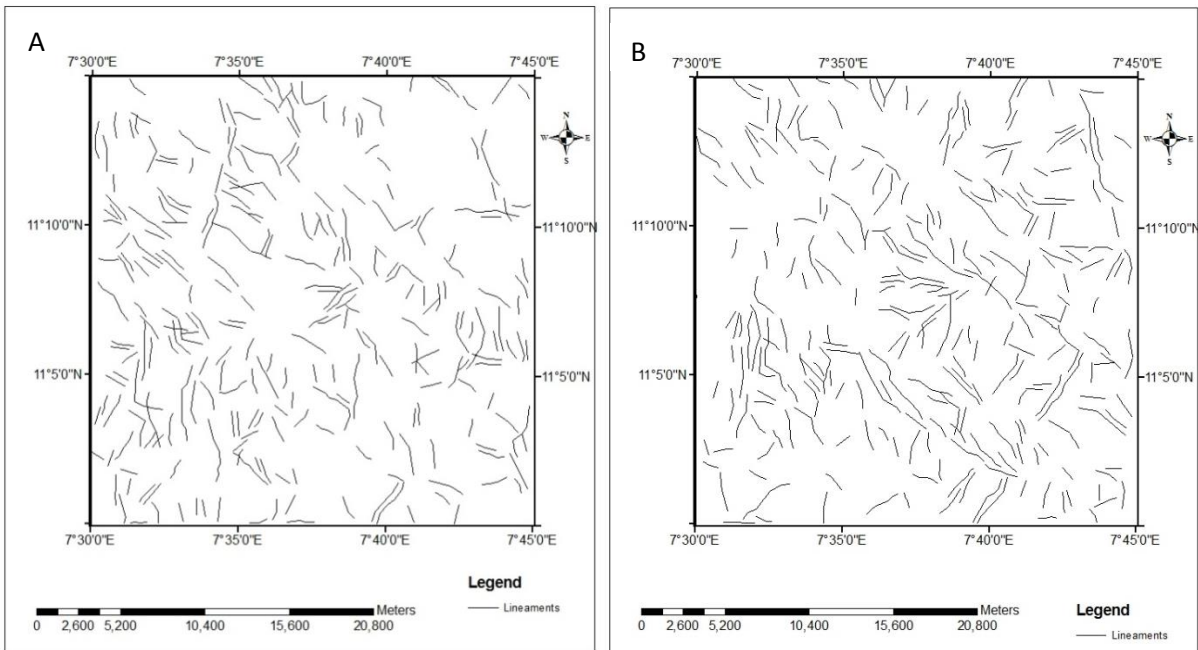
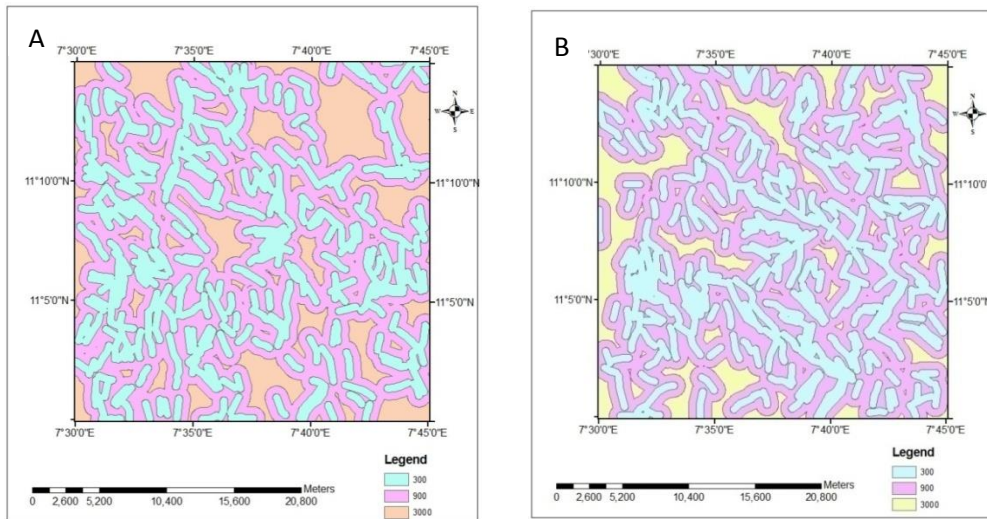


Figure 6: Automatically Generated Lineaments A = (0, 45, 90, 135), B = (180, 225, 270, 315) (from present work)

Buffering and Reclassification

After automatically generation of lineaments, buffering was performed, and reclassification of these buffered images was done (Figure 7).



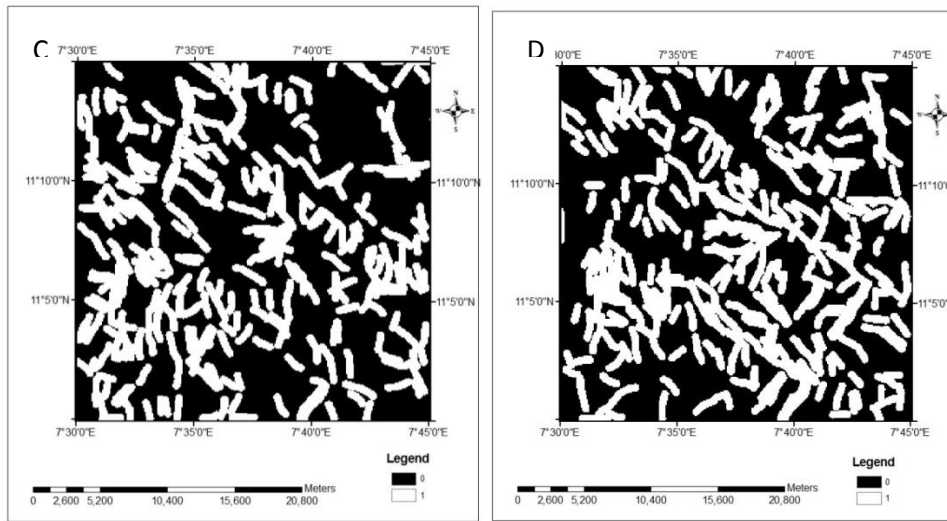


Figure 7: (A) Buffered Image 0, 45, 90, 135 (B) Buffered Image 180, 225, 270, 315 (C) Reclassified Buffered Image 0, 45, 90, 135, (D) Reclassified Buffered Image 180, 225, 270, 315

The reclassified buffered image was then combined to produce a level of coincidence image (Figure 8A). The level of coincidence image was then reclassified to produce a reclassified level of coincidence image (Figure 8B).

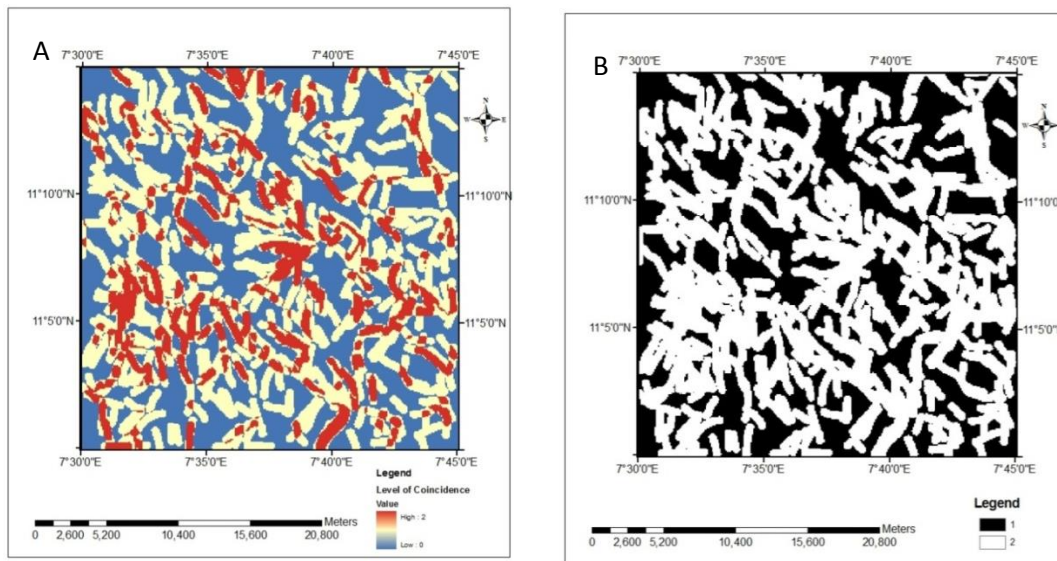


Figure 8: A = Level of Coincidence Image, B= Reclassified Level of Coincidence Image

From the level of coincidence image, manual digitization was carried out to produce a final lineament map (Figure 9).

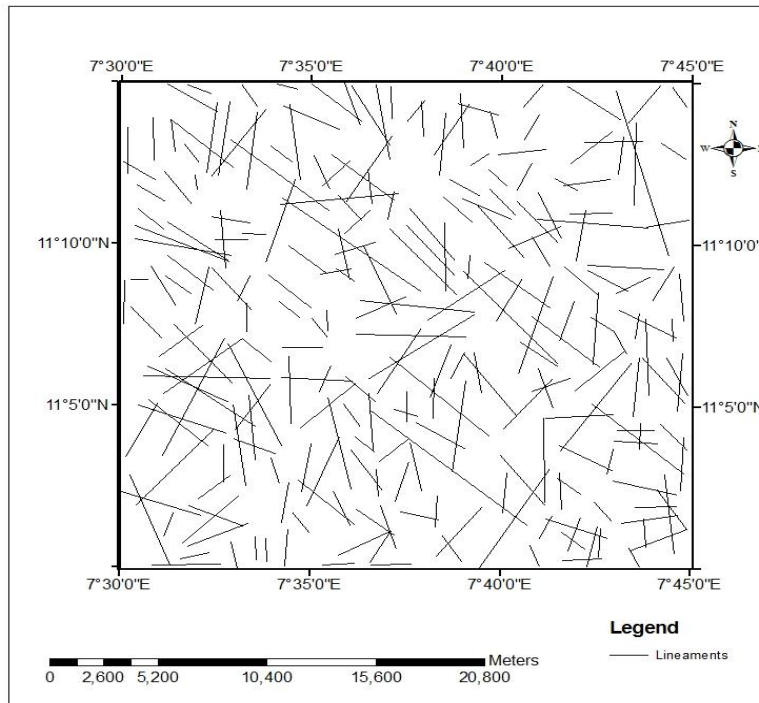


Figure 9: Final Lineament Map for the Study Area

Lineaments produced from both maps and the combined map had a dominant N-S and NW-SE direction accompanied by a less dominant NE-SW direction (Figure 10 and 11). A total of 248 lineaments were produced from the final lineament map.

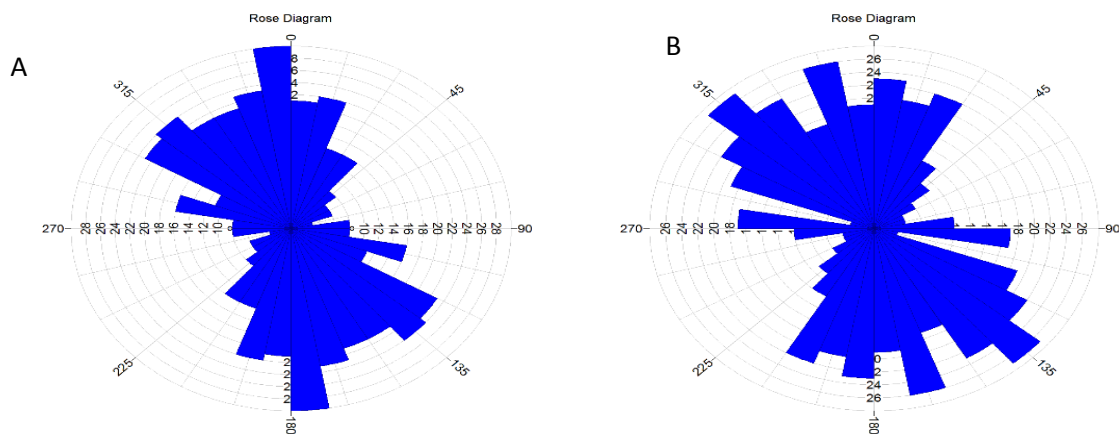


Figure 10: Lineament Directions for Study Area A= From Buffered Image 0, 45, 90, 135, B = 180,225,270,315

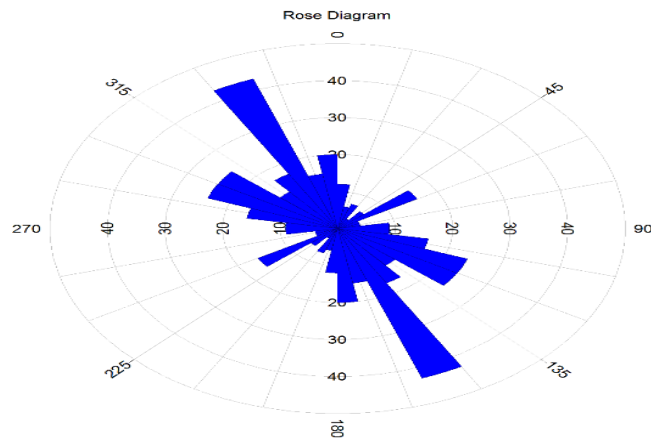


Figure 11: Final lineament orientation

Statistical orientation and lineament density analysis

Lineament length for the study area had a minimum of 0.8740km, a maximum of 10.0535km, a mean of 2.9510km and a standard deviation of 1.5497km. Histogram plot for lineament length shows a positive skew (Figure 12). Positive skewness for lineaments is an indication that most lineaments in the study area are not extensive.

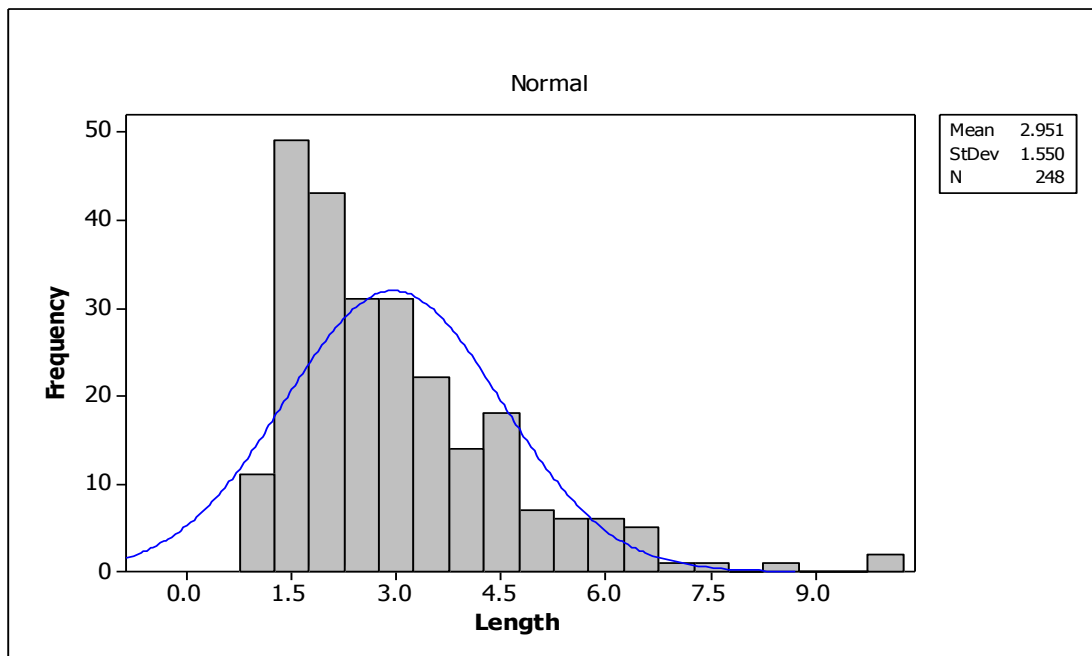


Figure 12: Histogram for Lineament Length

The lineament density calculates the number of lineaments per unit area. Lineament density aids in understanding the degree of shearing within the study area. Lineament density for the study area ranges from 0 to 32, with a mean of 0.9 and a standard deviation of 0.54. Areas of extremely high lineament density are located in the western part of the study area and constitute 0.38% of the study area, occupying an area extent of 2.90km². Areas of very high lineament density occur in the eastern to northern to south eastern part of the study area. It makes up 3.5% of the study area and has an area extent of 26.73km². Areas of high lineament density occur in the western, south eastern and central to northern part of the study area, occupying an area extent of 150.4 km² and covers 19.7% of the study area. Areas of low lineament density are papered throughout the study area, have an area extent of 329.2km² and constitute 43.1% of the study area. Areas of very low lineament density occurs throughout the study area, have an area coverage of 253.62 constitute 33.2% of the study area. (Figure 13)

Lineament Intersection Density

Lineament intersection density ranges from 0-6.767, with a mean of 0.267 and a standard deviation of 0.54. Areas depicted as having extremely high lineament intersection density are located in the southern parts of the study area, covers an areas of 0.012 km² representing 0.00158% of the study area. Areas of very high lineament intersection densities are located in the southern part of the study area. They represent 0.07% of the study area and have area coverage of 0.05km². Areas depicted as having high lineament intersection density are located in the western and south eastern part of the study area covers an area of 1.757km² representing 0.23% of the study area. Areas depicted as having low lineament intersection densities occurs in the Northern, eastern and south western part of the study area. It has areas coverage of 20.6km² representing 2.7% of the study area. Areas having very low lineament intersection density covers 96.9% of the study area and have an area coverage of 740.2km² (Figure 14).

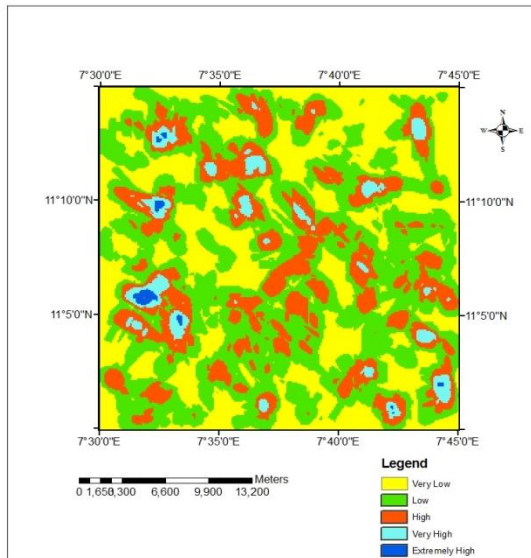


Figure 13: Lineament Density

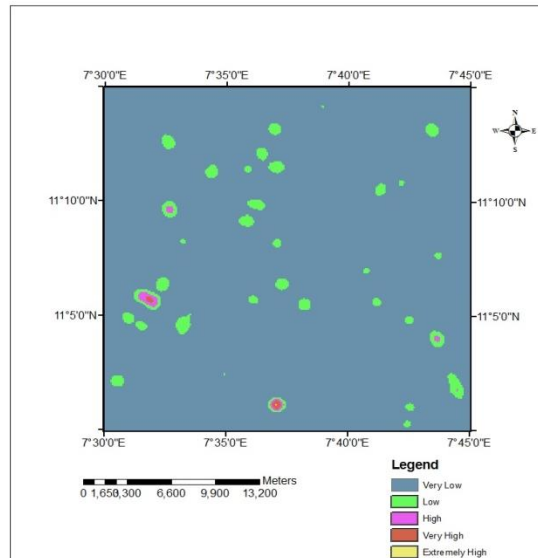


Figure 14: Lineament Intersection Density

Mean lineament length for the study area had a minimum of 0.6, a maximum of 3.9 and a mean of 1.5. Areas with extensive lineament length accounted for 6.9% and cover a surface area of 52.7km². Areas of long lineament length accounted for 28.5% of the study area and covers a surface area of 217.7km². Areas of short lineament length accounted for 50.7% of the study area and covers a total area of 387.3km². Areas of very short lineaments accounted for 13.7% of the study area and covers a total area of 104km². Areas of extensive lineaments are located in the central and western part of the study area. Areas of long lineaments are located in the central, North eastern and western part of the study area (Figure 15).

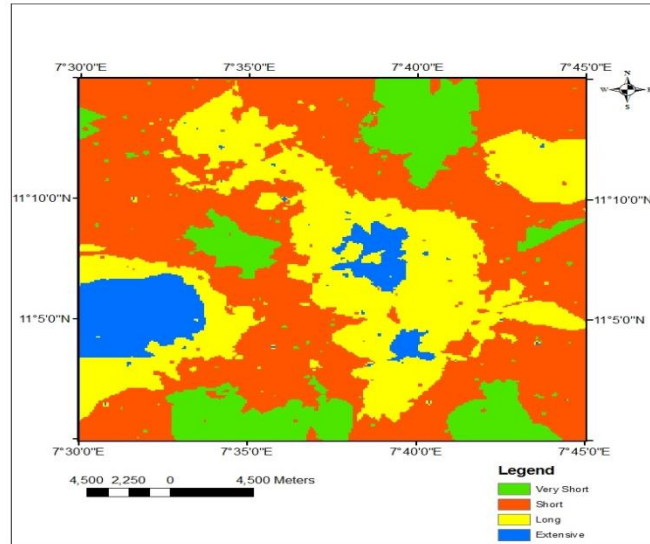


Figure 15: Mean Lineament Map

N-S lineament abundance has a minimum of 0, a maximum of 5.4, a mean of 0.08 and a standard deviation of 0.266. N-S relative lineament abundance was subdivided in to four classes. Areas with Very high N-S relative abundance accounted for 0.09% of the study area and have an area extent of 0.687km². Areas with high N-S relative abundance accounted for 1.39% of the study area and have an area extent of 9.93km². Areas with low N-S relative abundance accounted for 5.92% of the study area and have an area extent of 45.22km². Areas with Very low N-S relative abundance accounted for 92.5% of the study area and have an area extent of 706.6km². High relative abundance areas are located in the north western and south eastern part of the study area. High and low relative abundance are papered throughout the study area (Figure 16).

E-W lineament abundance has a minimum of 0, a maximum of 2.4, and a mean of 0.06 and a standard deviation of 0.21. N-S relative lineament abundance was subdivided in to four classes. Areas with Very high E-W relative abundance accounted for 0.07% of the study area and have an area extent of 0.53km². Areas with high E-W relative abundance accounted for 0.267% of the study area and have an area extent of 1.98km². Areas with low E-W relative abundance accounted for 4.3% of the study area and have an area extent of 32.8km². Areas with Very low E-W relative abundance accounted for 95.3% of the study area and have an area extent of 728km². High relative abundance area are located in the western part of the study area. High and low relative abundance are papered throughout the study area (Figure 17).

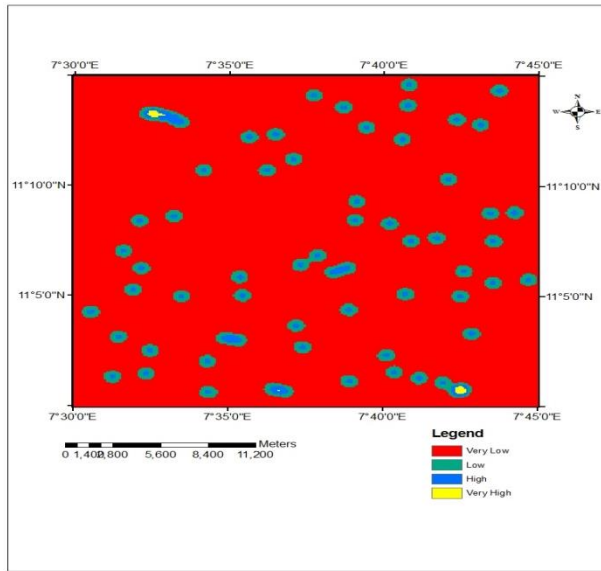


Figure 16: N-S Relative Abundance Lineament Map

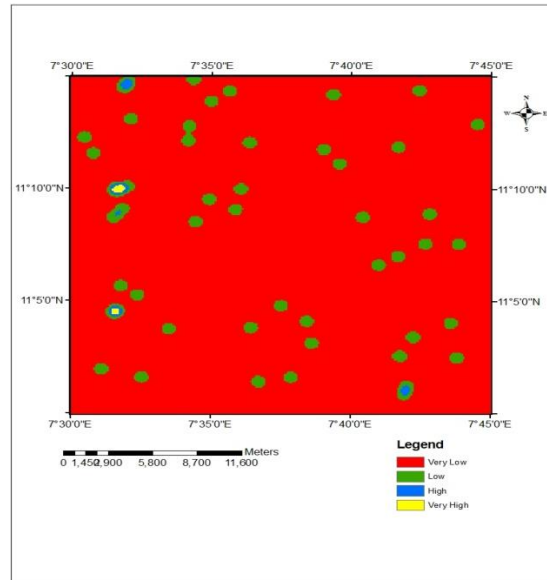


Figure 17: E-W Relative Abundance Lineament Map

NE-SW lineament abundance has a minimum of 0, a maximum of 1.8, and a mean of 0.043 and a standard deviation of 0.176. NE-SW relative lineament abundance was subdivided in to four classes. Areas with Very high NE-SW relative abundance accounted for 0.1% of the study area and have an area extent of 0.74km². Areas with high NE-SW relative abundance accounted for 1.24% of the study area and have an area extent of 9.43km². Areas with low NE-SW relative abundance accounted for 2.79% of the study area and have an area extent of 21.31km². Areas with Very low NE-SW relative abundance accounted for 95.7% of the study area and have an area extent of 731.0km². High relative abundance areas are located in the eastern and south western part of the study area. High and low relative abundances are papered throughout the study area (Figure 18).

NW-SE lineament abundance has a minimum of 0, a maximum of 2.1, a mean of 0.12 and a standard deviation of 0.86. NW-SE relative lineament abundance was subdivided in to four classes. Areas with Very high NW-SE relative abundance accounted for 0.2% of the study area and have an area extent of 1.52km². Areas with high NW-SE relative abundance accounted for 1.7% of the study area and have an area extent of 12.9km². Areas with low NE-SW relative abundance accounted for 8.5% of the study area and have an area extent of 64.93km². Areas with Very low NW-SE relative abundance accounted for 89.5% of the study area and have an area extent of 683km². High relative abundance areas are located in the central, southern and eastern of the study area. Low relative abundances are papered throughout the study area (Figure 19).

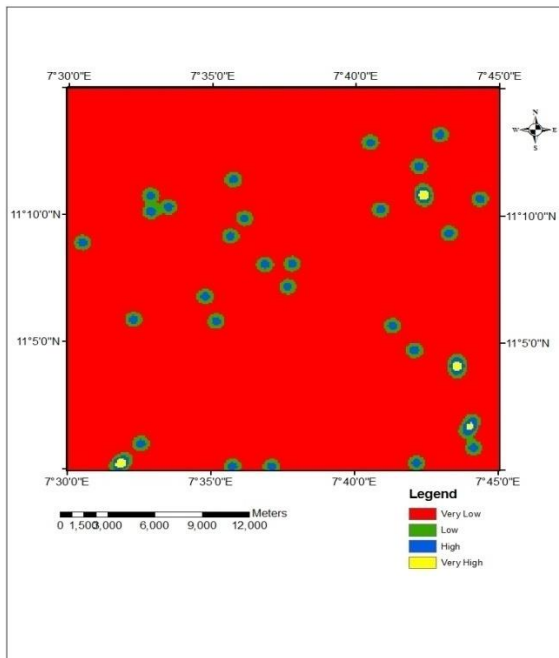


Figure 18: NE-SW Relative Abundance Map

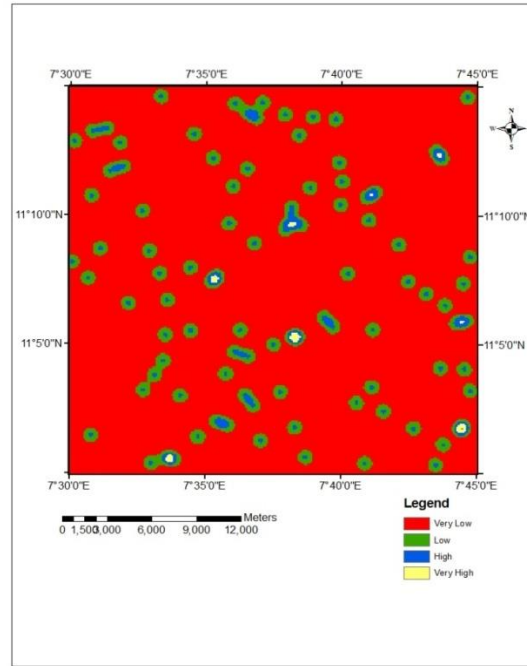


Figure 19: NW-SE Relative Abundance Lineament Map

Relationship between lineament length and Orientation

Relationship between mean length and azimuth was compared using tables and diagrams. Mean length for lineament orientation N-S, NW-SE, NE-SW, E-W was used for this analysis. From this comparison, it was observed that the NW-SE lineaments are the most abundant and the short lineament species are the most abundant. Using dendrogram in terms of length, we observed that the NW-SE and NE-SW lineaments are most correlating. Also the NE and E-W lineament species are more correlating than NW-SE and NE-SW lineaments (Figure 20 and 21).

Table 1: Relationship between Lineament Length and Orientation

	N-S	NW-SE	E-W	NE-SW	Total	%
Very Short	19	36	16	13	84	33.8
Short	43	57	32	20	152	61.2
Long	4	3	1	1	9	3.6
Very Long	0	1	2	0	3	1.2
Total	66	97	51	34	248	
%	26.6	39.1	20.5	13.7		

(From present work)

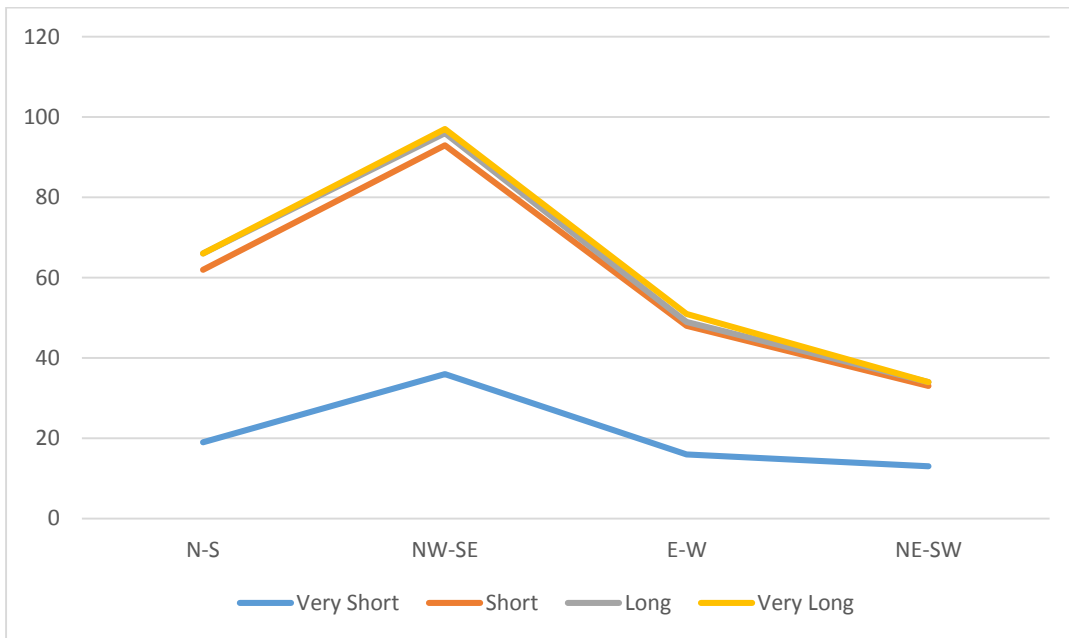


Figure 20: Correlation Plot for Lineament Species (From present work)

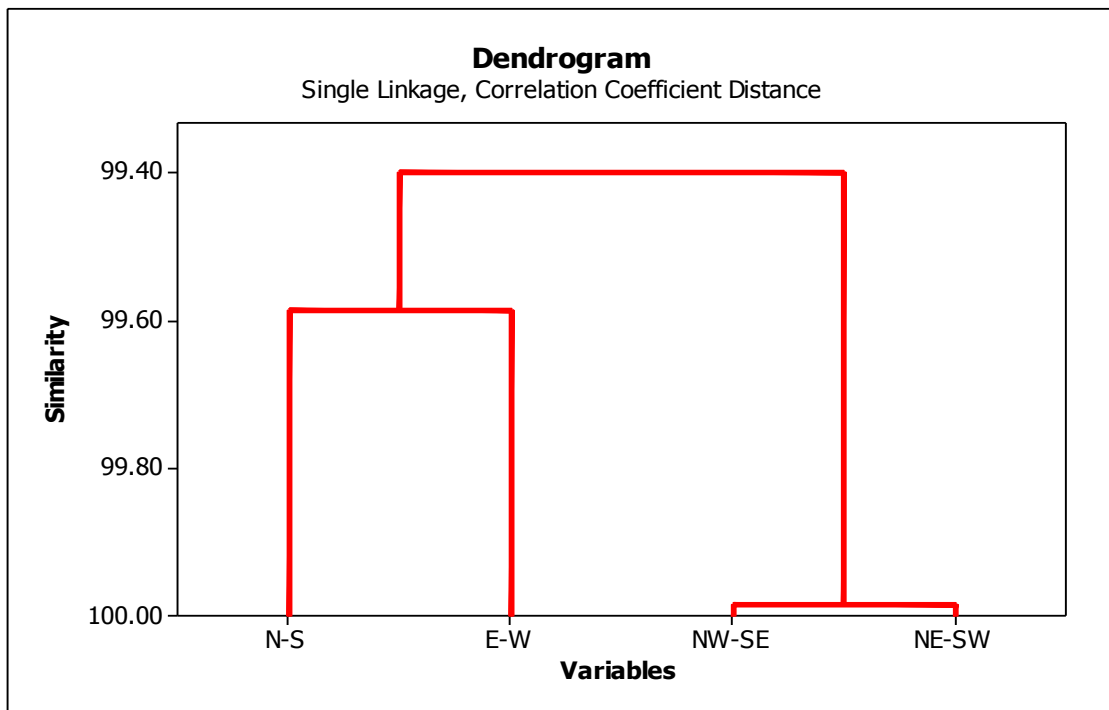


Figure 21: Dendrogram for Lineament Specie (From present work)

Lithological Mapping

A false colour composite for the study area was produced to map lithological variations within the study area. Band 741 was used to map lithological variations within the study area. Decorrelation stretch was applied to enhance variations in lithologies (Figure 22 and 23).

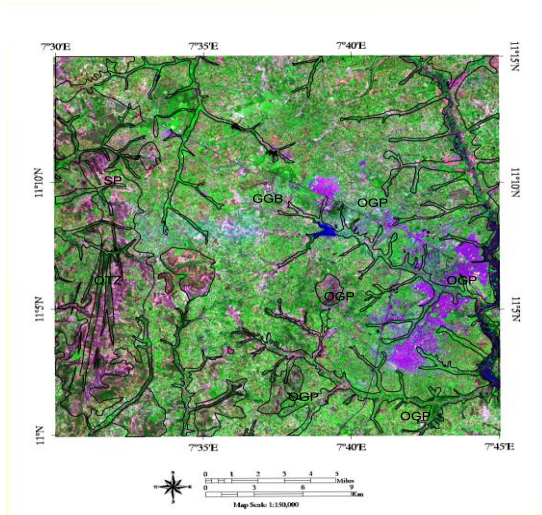


Figure 22: False Colour composite image 741

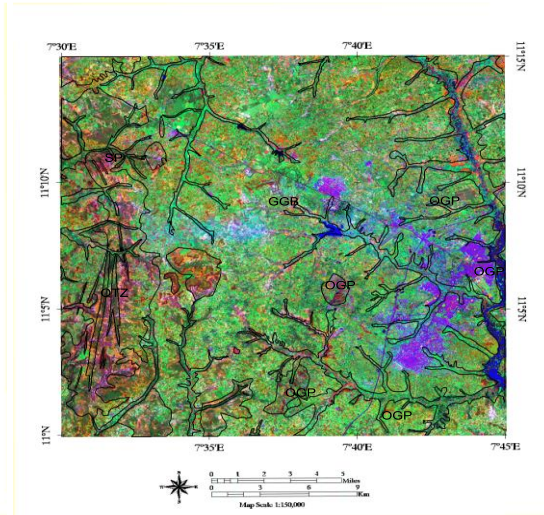


Figure 23: Decorrelation stretch of False Colour composite 741

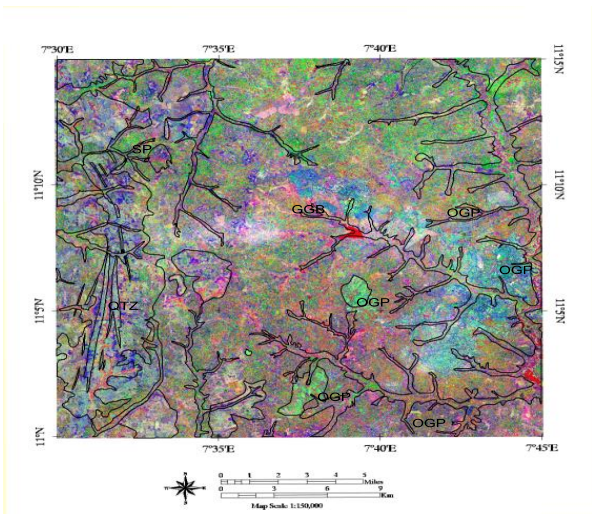


Figure 24: MNF 123 Image

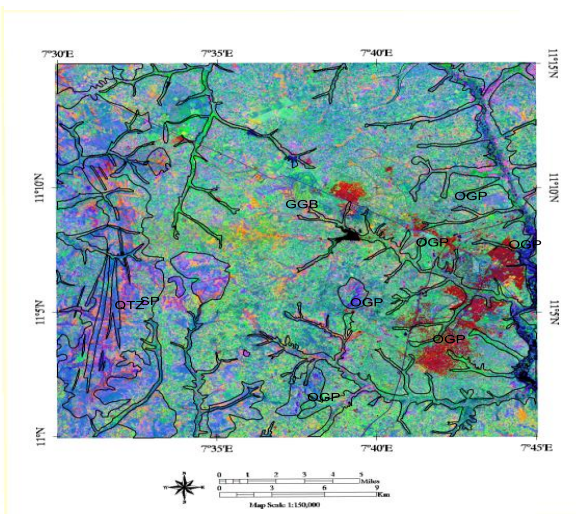


Figure 25: Principal Component Analysis Image for the Study Area

Legend:

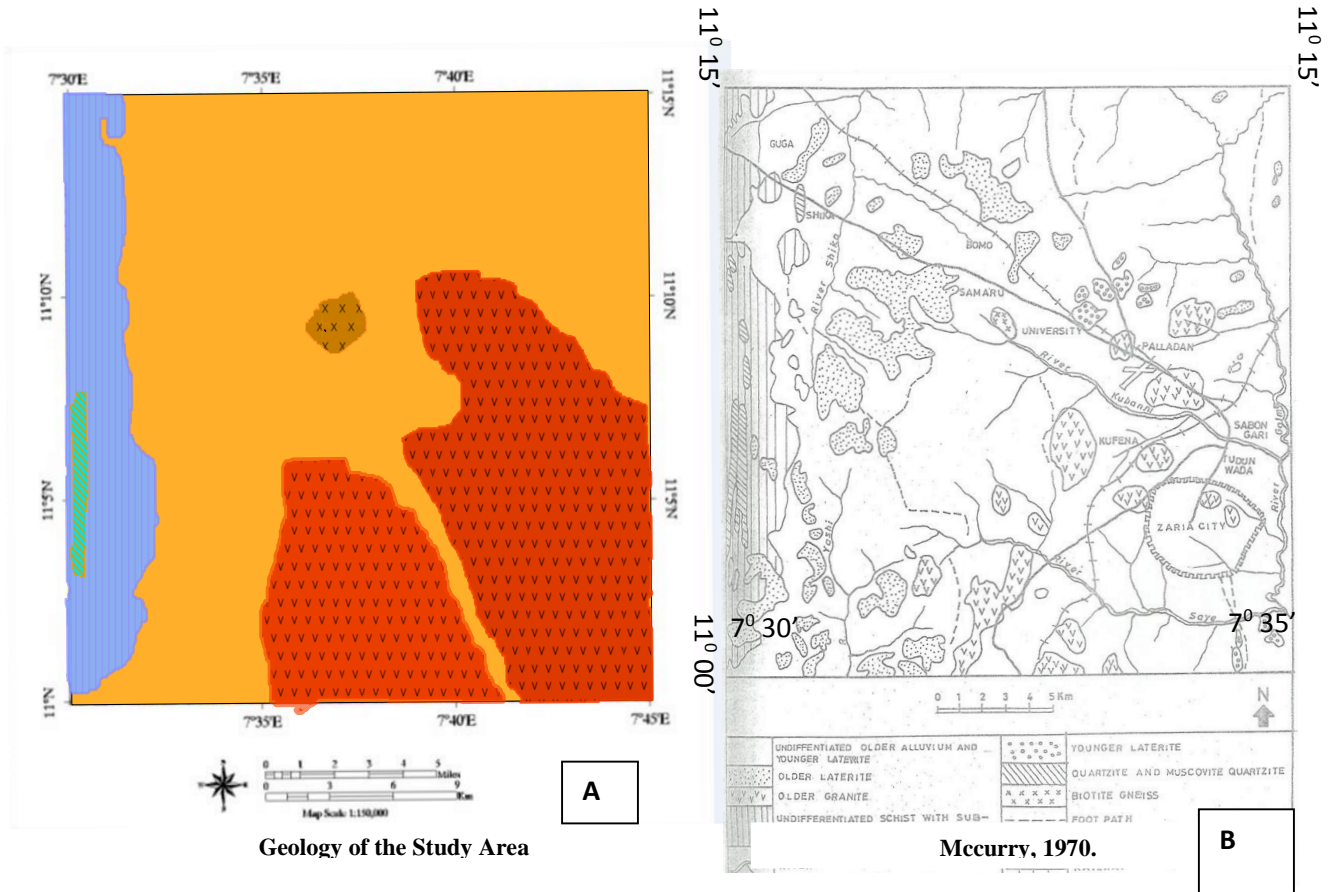
OGP = Porphyroblastic biotite granite

GGB = Biotite granite gneiss

SP= Semi pelitic schist and phyllite metasilstone, carbonataceous schist

QTZ = Quartzite and muscovite

I



LEGEND





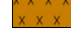
-  Undifferentiated Older Alluvium and Younger Laterite
-  Older Granite
-  Semi Pelitic Schist and Phyllite Metasiltstone, Carbonaceous Schist
-  Quarzite
-  Biotie Gneiss

Figure 26: Comparison between lithological maps from the present study (A) and that of McCurry, 1970 (B)

The final lineament and lithological map of the study area is given below in Figure.27.

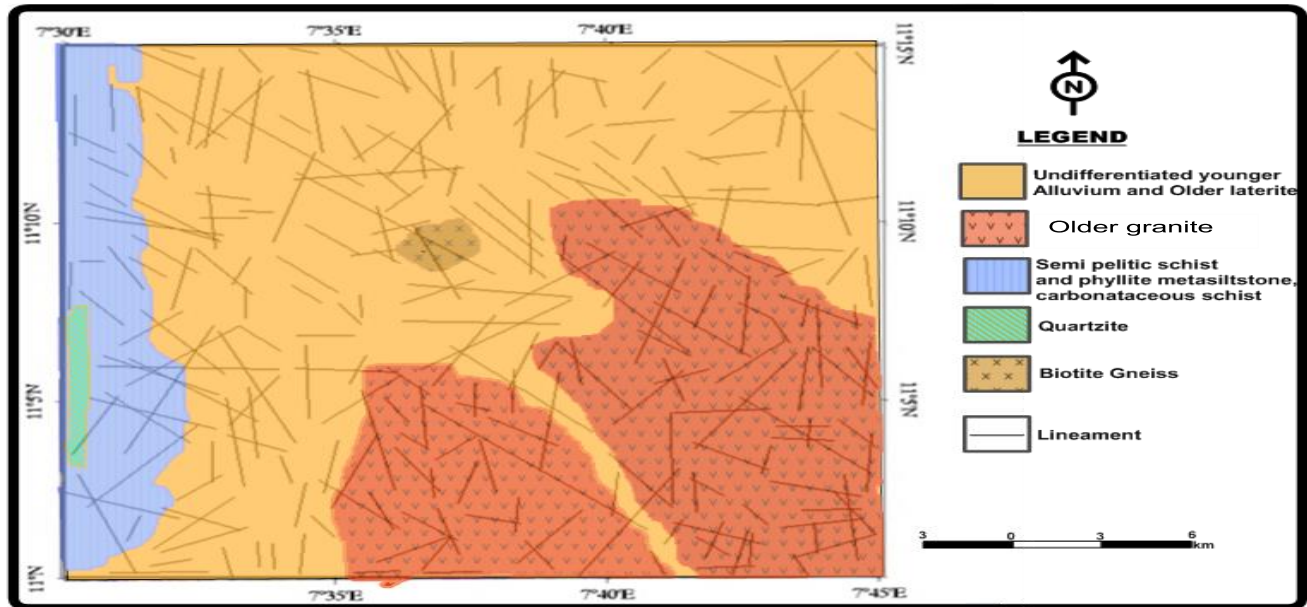


Figure 27: Geology and Lineament Map of the Study Area (From present study)

Zaria belongs to the Nigeria Basement Complex, which according to McCurry (1973) consists of four distinct rock types namely; the Basement Gneiss, Metasediments ranging from quartzite to schist, the Older Granite suites and diorite. Ratios of Landsat ETM+ bands played an important role in Landsat image interpretation and identification of different lithologies. However; there are three distinct lithologies within the study area. This comprises of the Older granite, gneiss and metasedimentary rocks. These results mean that the ratios have managed to some extent to evade the interference between vegetations and lithologies which have been reported from different studies example in Crosta and Moore (1989). Colour composite images 7:4:1 were used to further discriminate individual lithological unit (Figures 24 and 25) with reasonable degree of accuracy, individual rocks e.g. Older granites, Biotite gneiss and metasedimentary rocks (Figure 27) which is similar to that of McCurry and Wright (1970).

Final lineament map shows a total of 248 lineaments were produced from the final lineament map, most lineaments in the study area are not extensive.

CONCLUSION

Different processing techniques were applied to the Landsat ETM+ images to discriminate the lithological units, and lineaments. The Band rationing, Principal Component analysis and False Colour Composites allowed broad discrimination of lithologies. Band ratios and composite images have played a great role in discriminating and identifying different rock types. Results from this study suggest that large part of geological mapping can be done through the use of Landsat and additionally they are cheap compared to the geophysical data, sometimes these data are free.

Lineament analysis should be carried out using higher resolution satellite to compare the accuracy with low resolution satellites. There is no standard on selection of the optimum band for manual lineament extraction. Therefore, it is recommended that the geologic, topographic properties and vegetation cover of the selected area should be taken into consideration.

REFERENCES

- Assiri, A., Alsaleh, A. and Mousa, H. (2008). Exploration of Hydrothermal Alteration Zones Using ASTER Imagery: A case study on Nuqrah Area, Saudi Arabia. *Asian J. Earth Sci.* 2: 1819-1886.
- Carranza, E.J.M. (2002). *Geologically - Constrained Mineral Potential Mapping: Example from the Philippines*. International Institute of Aerospace Survey and Earth Science (ITC), PhD Thesis. 88: 1- 474.
- Carranza, E.J.M and Hale M. (1999). Image processing and GIS for hydrothermal alteration mapping, Baguio district, Philippines. Proceedings of the 1999 IEEE International Geoscience and Remote Sensing Symposium, Hamburg, Germany, 28 June-2 July.
- Crosta, A.P., De Souza Filho, C.R., Azevedo, F. and Brodie, C.(2003) Targeting key alteration minerals in Epithermal deposits in Patagonia, Argentina, using ASTER imagery and principal component analysis. *Int. J. Remote Sens.*24:4233-4240.
- Crosta, A.P and Moore, J.M. (1989) Enhancement of Landsat Thematic Mapper imagery for residual soil mapping in SW Minas Gerais state, Brazil: a prospecting case history in Greenstone belt terrain
- Drury, S.A (1993). *Image interpretation in Geology*, 2nd edition, Chapman & Hall Publishing Company, London. p.283.
- Ferrier, G., Griffiths, K.W.G., Bryant, R. and Stefouli, M. (2002). The mapping of hydrothermal alteration zones on the island of Lesbos, Greece using an integrated remote sensing dataset. *Int. J. Remote Sens.* 23:1-16.
- Ike, E.C. (1974). *The Structure, Petrology and Economic Geology of the Zaria Batholith*, Unpublished B.Sc. Project, Ahmadu Bello University, Zaria.
- Jensen, J.R (1996). *Introductory digital image processing: A Remote sensing perspective*, second ed, prentice Hall, saddle River, NJ,316pp.
- McCurry, P. (1970). *The Geology of the Degree Sheet 21*. Unpublished M. Sc. Thesis, Ahmadu Bello University, Zaria.
- McCurry, P. (1973). Geology of degree sheet 21, Zaria Nigeria.Oversea. *Journal of Geology and Mining Research*, 45,I.G.S London 45pp
- McCurry, P. (1976). The Geology of the Precambrian to Lower Paleozoic Rocks of Northern Nigeria, a review in Kogbe, C.A. (2nd edition), *Geology of Nigeria*. Elizabethan, Publ. Co. Lagos. pp 13- 37.

Moore, C.A., Hoffmann, G.A. and Glenn, N.A. (2007). Quantifying basaltic rock outcrops in NRCS Soil Map Units Using Landsat-5 Data. *Soil Surv. Horiz.* 48: 59-63.

Olunsiyi, S.A. (2013). Geology and structure of pre cambrian rocks in Iworoko, Are, and Afao area, south western Nigeria. *International Research Journal of Natural Sciences* 1, 14-29.

Oyawoye, M.O. (1964). *The Basement Complex of Nig. African Geology*. University of Ibadan Press.

Woakes, M., Rahaman, M.A. and Ajibade, A.C. (1987). Some Metallogenic features of Nigerian Basement. *Journal African Earth Sciences*, 6:54-56.